Modelling the constrained recovery in shape memory wires

Mattia Merlin, Raffaella Rizzoni
Department of Engineering, University of Ferrara, Italy
E-mail: mattia.merlin@unife.it, raffaella.rizzoni@unife.it

Keywords: shape memory wires, constrained recovery, smart composites.

SUMMARY. The first part of this paper reports a one-dimensional model, proposed in [1], for simulating the microstructural evolution of phase transforming thin wires in uniaxial constrained recovery conditions. The model can explain the shift to higher transformation temperatures observed in experiments on shape memory wires [2, 3, 4, 5]. The effect of increasing the pre-straining on the evolution of the recovery stress and on the martensite volume fraction can also be captured [6, 7]. In the second part of the paper, we report a work that is still in progress [8], in which we apply the model in order to study a composite with shape memory wires. The model is able to qualitatively reproduce the deformation of a prototype realised in the Laboratory of Metallurgy of the Department of Engineering at the University of Ferrara.

1 INTRODUCTION

Shape memory alloys are characterised by a reversible, diffusionless, solid-solid phase transformation between two different crystal configurations (known as *austenite* and *martensite*). At temperatures lower than a pre-defined critical temperature θ_{cr}, the alloy exists in the martensite phase. In this phase, the material can be deformed into any arbitrary shape with strains up to 8%. When the alloy is heated over θ_{cr}, it begins to transform back into the austenite or parent phase. During the reverse transformation from martensite to austenite, the material returns to the pre-deformed shape. After that, if the temperature falls under θ_{cr} once again, the alloy goes into direct, austenite to martensite transformation. In direct transformation the specimen shape remains unchanged until an external force is applied. The recovering of the original shape upon heating is known as the shape memory effect.

The constrained shape memory effect is observed when an external constraint prevents the material from returning to the shape it had in the parent phase. For example, in shape memory wires embedded or bonded to an elastic matrix, shape recovering induced by phase transformation is restricted by the matrix. In this situation, large recovery stresses, up to 700 MPa, are generated [3].

Several studies propose constitutive phenomenological models able to reproduce the macroscopic response of shape memory materials in constrained recovery conditions [9, 10, 11, 6, 2] and in shape memory composites [12, 13, 14]. However, recent experimental work shows that the evolution of the material microstructure plays an important role in the mechanism at the basis of the recovery stress generation. In fact, several studies have established that, for pre-strained NiTi fibres, the reverse (from martensite to austenite) transformation is spread over a much wider temperature range than the transformation of a fibre in free conditions [2, 4]. Zheng et al. attributed this phenomenon to microstructure evolution, in particular to the transformation of preferentially oriented martensite variants [5].

In Section 2, we present a one-dimensional model developed in [1], which can simulate the microstructural evolution of a phase transforming single crystal thin wire. The model is based on the *constrained theory of martensite* [15, 16, 17]: stable equilibrium configurations are found among deformations lying at the energy wells on most part of the wire and minimise the free energy of the

material. Notably, the input parameters of the model are a small number of fundamental material constants. On the other hand, the hysteretic behaviour typical of shape memory materials is not captured. In fact, hysteresis is commonly believed to be associated with metastable states and therefore with local minimisers of the total energy while in [1] we identify stable equilibrium configurations with *global* minimisers.

In Section 3 we summarise the results of the analysis of the uniaxial constrained recovery performed in [1] by using the model presented in Section 2. These results theoretically confirm Zheng's observations. They can also explain the effect of pre-straining and the matrix stiffness on the evolution of the recovery stress reported in [6, 7].

Smart composites incorporating pre-strained shape memory wires are becoming more and more popular for shape and position control of structural elements (see [18] and the reference therein). Important performance parameters for such smart components include those associated with the geometry and the transforming characteristics of wires, such as diameter, pre-straining and transformation temperature, and those associated with matrix, such as thickness and stiffness. The interplay between all these quantities must be taken into account. For example, a minimum level of matrix rigidity is required not only to return the actuated composite to its original position but also to pre-strain the embedded wires again for the next cycle. On the other hand, excessive rigidity of the matrix could become difficult to overcome when trying to achieve the desired deformation.

To understand this and related issues, we have undertaken a study of the deformation of a composite made of a shape memory wire attached to a thin elastic isotropic plate [8]. The thermomechanical behaviour of the wire is described by the model presented in Section 1. The plate is assumed to deform according to the classical small-deformation Kirchhoff theory. We write the total potential energy of the system and we invoke the principle of stationary potential energy to determine optimal values of the deformation parameters involved. These give elementary formulae for the relationships between the in-plane strains and curvatures of the layer and the wire temperature. These formulae qualitatively describe the deformation of a prototype realised in the Laboratory of the Department of Engineering at the University of Ferrara.

2 A ONE DIMENSIONAL MODEL FOR PHASE TRANSFORMING THIN WIRES

Let $\omega \subset \mathbb{R}^2$ be an open bounded domain with Lipschitz boundary and unit area, which we identify with the cross-section of the wire, and let $\omega \times (0, L)$ be the reference, undeformed configuration of the wire. We introduce a coordinate system so that the x_3-axis coincides with the undeformed wire axis and we denote e_3 the x_3-axis unit vector. If $L \gg 1$, i. e. if the wire is very thin, its deformation can be approximately described by the deformation field $y : (0, L) \mapsto R^3$ of its centre line [19].

We assume that the wire is in the austenitic phase in the reference configuration and we introduce the sets of the austenite and of the martensite wells, respectively, defined as

$$A := SO(3) \ , \quad M =: \bigcup_{i=1}^{N} \{QU_i : Q \in SO(3)\}, \tag{1}$$

where $SO(3)$ is the set of all proper rotations and $U_1, U_2, \ldots U_N$ denote N symmetric and positive definite 3×3 matrices describing the transformation strains from austenite to the martensite variants [20]. The microstructure of the material is described by a family of Young measures $x_3 \mapsto \nu_{x_3}, x_3 \in (0, L)$, supported on $A \cup M$ and the macroscopic deformation gradient is viewed as the centre of

mass of the Young measure:

$$y_{,3}(x_3) = \int_{A\cup M} Fe_3 \, d\nu_{x_3}(F) \ , \quad \text{a.e. } x_3 \in (0, L). \tag{2}$$

Thus a couple (ν_{x_3}, y) completely describes a configuration of the wire, in the sense that it embeds information both on the microstructure and on the macroscopic configuration.

The stable equilibrium configurations of the wire are assumed to globally minimise the energy

$$E((\nu, y); \theta) = \int_0^L \left(l_m(\theta) \int_M d\nu_{x_3}(F) + l_a(\theta) \int_A d\nu_{x_3}(F) \right) dx_3, \tag{3}$$

where $l_a(\theta)$, $l_m(\theta)$ are the bottom levels of the austenite well and of the martensite wells at temperature θ, respectively. To model the exchange of global minimum between austenite and martensite occurring in a temperature change, we take $\Delta l(\theta) := l_m(\theta) - l_a(\theta)$ a monotonic increasing function in θ, vanishing at θ_{cr}. The derivative $\Delta l'(\theta_{cr})$ can be shown to be related to the latent heat of the phase transformation and, for simplicity, we assume a linear dependence of $\Delta l(\theta)$ from θ near θ_{cr}

$$\Delta l(\theta) \approx \frac{q\rho}{\theta_{cr}}(\theta - \theta_{cr}), \tag{4}$$

with ρ the density of the material and q the latent heat of transformation per unit mass.

It is interesting to note that the input parameters of the model are a small number of fundamental material constants: the Bain transformation matrices $U_1, U_2, \ldots U_N$, of which the components can be obtained from X-ray measurements of lattice parameters of parent and product phases; the equilibrium transformation temperature θ_{cr}; the density of the material ρ and the latent heat of transformation q. Both the transformation temperature and the latent heat can be obtained from differential scanning calorimetry measurements.

3 UNIAXIAL CONSTRAINED RECOVERY

Consider a wire of length L in the austenitic state (Fig. 1.a) and deformed in the martensitic state by an uniaxial extension of amount $\epsilon_c > 0$ (Fig. 1.b). To study the constrained shape memory effect, we suppose that the wire is then bonded to a linear elastic spring of stiffness k and the system ends are assumed to be fixed on heating to a temperature $\theta > \theta_{cr}$ (Fig. 1.c). In the latter configuration, the wire partially recovers its pre-straining ϵ_c, the spring deforms and stress is generated.

For each value of the temperature θ, the equilibrium configuration of the wire are the global minimisers of the total energy

$$E_k((\nu, y); \theta) = \int_0^L \left(l_m(\theta) \int_M d\nu_{x_3}(F) + l_a(\theta) \int_A d\nu_{x_3}(F) \right) dx_3 + \frac{1}{2} k d^2 \tag{5}$$

among the couples (ν, y) satisfying (2) and the boundary conditions

$$y(0) = 0 \ , \quad L(1 + \epsilon_c) = y(L) \cdot e_3 + d, \tag{6}$$

with $d > 0$ denoting the spring deformation. To describe the form of the minimiser, we now introduce some notation. We denote

$$\eta_i = \frac{1}{L} \int_0^L \int_{SO(3)U_i} d\nu_{x_3}(F), \ \ _1 = 1, 2, \ldots N \tag{7}$$

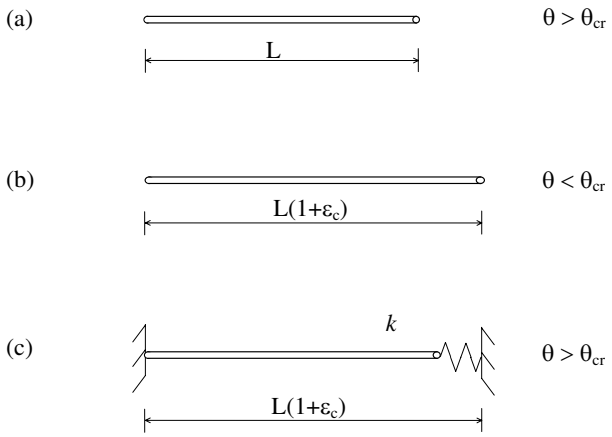

Figure 1: Constrained recovery: (a) initial, reference configuration of the wire (austenitic state), (b) deformed configuration of the wire after imposing pre-straining below the transformation temperature θ_{cr} (martensitic state) and (c) final configuration of the wire attached to a linear spring and heated above θ_{cr} (with the material given by a mixture of martensite and austenite).

the volume fraction of the $i-$th martensite variant and

$$\lambda = \sum_{i=1}^{N} \eta_i \tag{8}$$

the total martensite volume fraction. We also introduce the strain associated to the $i-$th martensite variant

$$\gamma_i = \mid U_i e_3 \mid, \;\; i = 1, 2, \ldots N, \tag{9}$$

and we denote

$$\gamma_M = \max\{\gamma_i \;:\; i = 1, 2, \ldots N\} \tag{10}$$

the maximum strain. Note that the martensite variant achieving the maximum may not be unique. We will call *preferentially oriented* martensite variants those variants achieving the maximum in (10).

In [1], we find that three types of qualitatively different minimisers occur, depending on the temperature.

- $\theta < \theta_{cr}$. A unique minimizer (ν_{x_3}, y) exists with the wire deformation given by

$$y(x_3) = (1 + \epsilon_c) x_3 e_3, \tag{11}$$

  and microstructure given by the family of Young measures

$$\nu_{x_3} = \sum_{i=1}^{N} \eta_i \delta_{Q_i U_i}, \quad x_3 \in (0, L) \tag{12}$$

with δ denoting the Dirac mass centered at Q_iU_i and the rotations $Q_i \in SO(3), i = 1, 2, \dots N$ chosen such that $Q_iU_ie_3 = \gamma_i e_3$. In (12), the volume fractions $\eta_i, i = 1, 2, \dots N$ are chosen to be the solution of the algebraic constrained problem:

$$\begin{cases} \sum_{i=1}^{N} \gamma_i \eta_i = 1 + \epsilon_c \\ \eta_i \geq 0, i = 1, 2, \dots N, \\ \sum_{i=1}^{N} \eta_i = 1 \, . \end{cases} \tag{13}$$

- $\theta = \theta_{cr}$. A family of minimizers exist. The wire deformation can be any element of the family of deformations

$$y(x_3) = (\lambda + \epsilon_c) x_3 e_3, \tag{14}$$

parameterized by $\lambda \in (\epsilon_c(\gamma_M - 1)^{-1}, 1)$. The microstructure is given by the family of Young measures

$$\nu_{x_3} = \sum_{i=1}^{N} \eta_i \delta_{Q_iU_i} + (1 - \lambda)\delta_I, \quad x_3 \in (0, L) \tag{15}$$

with I the identity matrix. The rotations Q_i are chosen as in the previous case and the volume fractions $\eta_i, i = 1, 2, \dots N$ are now chosen to be the solution of the algebraic constrained problem:

$$\begin{cases} \sum_{i=1}^{N} \gamma_i \eta_i = \lambda + \epsilon_c \\ \eta_i \geq 0, i = 1, 2, \dots N, \\ \sum_{i=1}^{N} \eta_i = \lambda \, . \end{cases} \tag{16}$$

- $\theta > \theta_{cr}$. A unique minimizer (ν_{x_3}, y) with y and ν_{x_3} still given by (14) and (15) evaluated at

$$\lambda = \frac{\epsilon_c}{\gamma_M - 1} - \frac{\Delta l(\theta)}{kL(\gamma - 1)^2}, \tag{17}$$

respectively.

By putting together these results and the estimate (4), we can predict the evolution of the martensite volume fraction λ with the temperature. As the temperature increases, the material, initially made of a mixture of martensite variants, changes to a mixture of austenite and martensite. In Fig. 2, the effect of increasing the pre-straining ϵ_c (Fig. 2.a) and the effect of increasing the spring stiffness k (Fig. 2.b) are shown. Notably, at $\theta = \theta_{cr}$ the martensite volume fraction displays a discontinuity from the initial value 1, corresponding to a mixture of martensite variants, to the value $\epsilon_c(\gamma_M - 1)^{-1}$. This drop corresponds to the transformation of the martensite variants not preferentially oriented into austenite. This is accompanied by a null macroscopic deformation of the wire. Note that the predicted volume fraction λ is continuous at $\theta = \theta_{cr}$ only when $\epsilon_c = \gamma_M - 1$. This is the maximum strain recoverable by the wire and in this case all martensite present in the configuration depicted in Fig. 1.b is made of preferentially oriented variants.

The discontinuity of the martensite volume fraction at θ_{cr} may explain the sudden drop of the martensite fraction observed in experimental martensite fraction/temperature profiles obtained from electrical resistivity measurements [6], differential scanning calorimetry measurements [2, 4] and X-ray diffraction results [5]. In [5], this drop is explicitly associated with the transformation of the not preferentially oriented martensite variants into austenite.

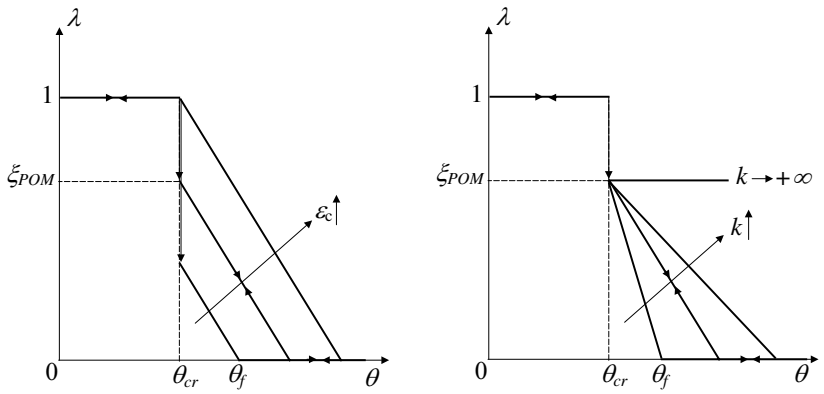

Figure 2: Evolution of the martensite volume fraction during constrained recovery: a) effect of increasing pre-straining; b) effect of increasing spring stiffness.

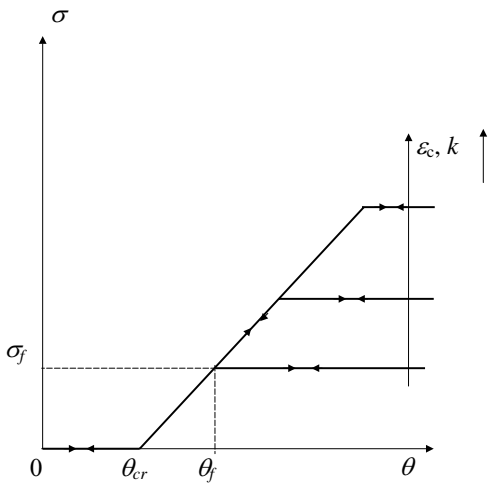

Figure 3: Evolution of the stress during constrained recovery.

Notably, our results predict the existence of the transformation temperature range (θ_{cr}, θ_f) for the preferentially oriented martensite. Using (4) and (17), we can calculate the temperature θ_f at which all the preferentially oriented martensite variants have been transformed into austenite:

$$\theta_f = \theta_{cr}(1 + \frac{kL(\gamma_M - 1)}{q\rho}\epsilon_c) \ . \tag{18}$$

This results agrees with the experimental evidence of a temperature range for the preferentially oriented martensite [2, 4, 5].

The stress-temperature profile, which can be evaluated using Hooke's law and (4), (6), (11), (14), (17), is represented in Fig. 3. The stress linearly increases starting from zero at θ_{cr} and reaching a saturation level σ_f at θ_f. As illustrated in Fig. 3, the stress σ_f increases as pre-straining and spring stiffness increases. Experimental observations qualitatively confirm these results [6, 7].

4 DEFORMATION CONTROL OF ELASTIC THIN LAYERS

We consider a layer of in-plane dimensions l_1, l_2 and thickness h upon which a shape memory wire is attached. We choose a rectangular coordinate system oriented as shown in Fig. 4, so that the direction z is normal to the plane of the layer with $z = 0$ lying in the midplane of the layer. As before, e_3 denotes the direction of the wire axis and we let α denote the inclination angle of the wire from the $x-$axis.

Before being attached to the layer at its extremities, the wire has been pre-strained of an amount ϵ_c in the martensitic state (as sketched in Fig. 1.b). Our goal here is to calculate the layer deformation as the temperature of the wire is increased above θ_{cr}.

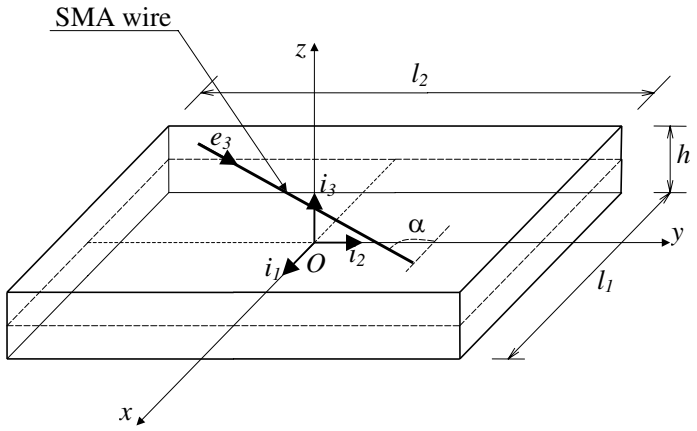

Figure 4: Orientation of the rectangular coordinate system with respect to the layer and to the wire.

In [8] the layer deformation is analysed under the following assumptions:

- the layer deforms according to the Kirchhoff hypothesis of thin plate theory, with the additional assumption that the normal stress components σ_{zz} vanishes everywhere;
- the displacements and all components of the displacement gradient tensor are small compared to unity so that the linear theory of elasticity can be applied;
- the in-plane strains are uniform extensions ϵ_x, ϵ_y along the axes x and y, respectively, and a uniform shear ϵ_{xy};
- the three midplane curvatures, denoted κ_x, κ_y and κ_{xy}, are spatially uniform;
- the material of the layer is linearly elastic and isotropic with Young's modulus E and Poisson's ratio ν;
- free edge effects and stress concentration in the layer due to load transfer between the wire and the layer are neglected;
- heat transfer between the wire and the layer is neglected and the wire temperature is assumed to be spatially uniform.

Under these assumptions, the layer energy can be expressed in terms of the corresponding strain components as follows:

$$\begin{aligned} E_L(\epsilon_x, \epsilon_y, \epsilon_{xy}, \kappa_x, \kappa_y, \kappa_{xy}) &= \frac{E}{2(1-\nu^2)} l_1 l_2 h(\epsilon_x^2 + \epsilon_y^2 + 2\nu\epsilon_x\epsilon_y + 2(1-\nu)\epsilon_{xy}) \\ &\quad + \frac{E}{24(1-\nu^2)} l_1 l_2 h^3(\kappa_x^2 + \kappa_y^2 + 2\nu\kappa_x\kappa_y + 2(1-\nu)\kappa_{xy}). \end{aligned} \tag{19}$$

The total potential energy of the system, given by the sum of (19) and the wire energy (3), depends upon the deformation field y of the wire centre line, the family of Young measure $x_3 \in (0, L), \nu_{x_3}$ describing the wire microstructure and the layer strain components $\epsilon_x, \epsilon_y, \epsilon_{xy}, \kappa_{xx}, \kappa_{yy}, \kappa_{xy}$. The stable equilibrium configurations of the system are identified with the solution of constrained minimisation of the total potential energy. The constraints which have to be taken into account in the minimisation are (2) and the continuity conditions of the displacement components at the extremities of the wire. In [8] it is shown that, in view of the assumptions listed above, the latter conditions reduce to the single condition

$$(\epsilon_x + \kappa_x \frac{h}{2}) \cos^2\alpha + (\epsilon_y + \kappa_y \frac{h}{2}) \sin^2\alpha - (\epsilon_{xy} + \kappa_{xy} \frac{h}{2}) \sin 2\alpha = \frac{1}{L} \int_0^L y_{,3} \cdot e_3 dx_3 - \epsilon_c. \tag{20}$$

In [8] we show that when $\theta > \theta_{cr}$ the strain components at equilibrium are

$$\epsilon_x = \xi \frac{\Delta l(\theta)}{E(\gamma_M - 1)} (\nu \sin^2\alpha - \cos^2\alpha), \tag{21}$$

$$\epsilon_y = \xi \frac{\Delta l(\theta)}{E(\gamma_M - 1)} (\nu \cos^2\alpha - \sin^2\alpha), \tag{22}$$

$$\epsilon_{xy} = \xi \frac{\Delta l(\theta)}{E(\gamma_M - 1)}(1+\nu)\sin\alpha\cos\alpha, \tag{23}$$

$$\kappa_x = 6\xi \frac{\Delta l(\theta)}{Eh^2(\gamma_M - 1)}(\nu\sin^2\alpha - \cos^2\alpha), \tag{24}$$

$$\kappa_x = 6\xi \frac{\Delta l(\theta)}{Eh^2(\gamma_M - 1)}(\nu\cos^2\alpha - \sin^2\alpha), \tag{25}$$

$$\kappa_{xy} = 6\xi \frac{\Delta l(\theta)}{Eh^2(\gamma_M - 1)}(1+\nu)\sin\alpha\cos\alpha, \tag{26}$$

with ξ the ratio of wire volume to layer volume. When $\theta > \theta_{cr}$ the total martensite volume fraction is still given by (17) with $k = l_1 l_2 h L^{-2} E$. The martensite fraction evolution with temperature displays the same features depicted in Fig. 2.

In Fig. 5 we compare the layer deformation predicted by the relations (21)-(26) with the deformation observed on a prototype developed in the Laboratory of Metallurgy of the Department of Engineering at the University of Ferrara. The prototype is a polymeric layer, onto which a pre-strained NiTi strip is attached. As the temperature of the strip is increased above the transformation temperature via ohmic heating, the strip recovers part of the pre-straining and the polymeric layer is seen to deform. Under the assumption that the strip works in traction, we model the strip as a wire. The predicted layer midplane deformation, estimated on the basis of relations (21)-(26) and depicted on the right-hand side of Fig. 5, qualitatively reproduces the prototype deformation, shown on the left-hand side of Fig. 5.b. Further details on the prototype and on its behaviour can be found in [8].

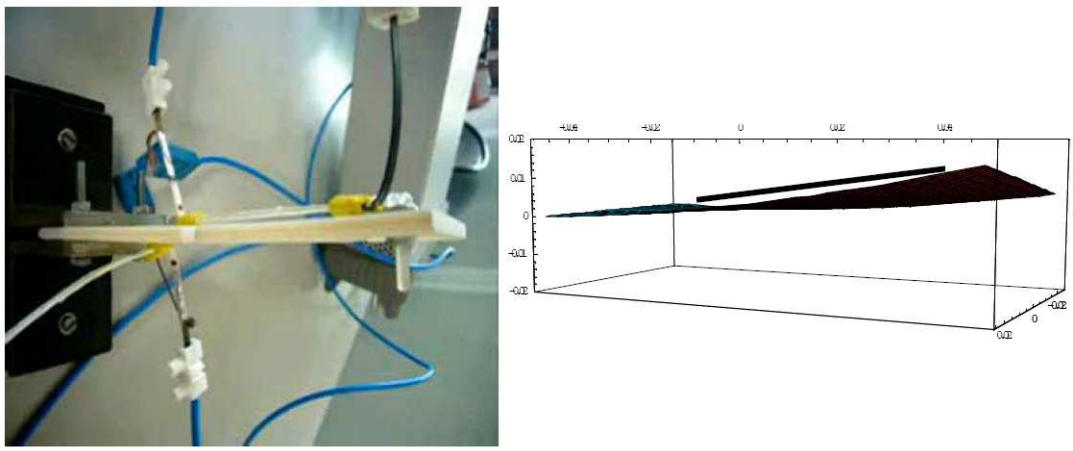

Figure 5: Prototype deformation under wire heating (left) and simulated deformation of the layer midplane at temperature above the transformation temperature (right).

References

[1] Rizzoni R., "A constrained theory for single crystal shape memory wires with application to restrained recovery," preprint (2009).

[2] Tsoi K. A., Stalmans R. and Schrooten J., "Transformational behaviour of constrained shape memory alloys," *Acta Mater.*, **50**, 3535–3544 (2002).

[3] Tsoi K. A., Schrooten J., Zheng Y. and Stalmans R.,"Thermomechanical characteristics of shape memory alloy composites," *Mater. Sci. Eng. A*, **368**, 299–310 (2004).

[4] Zheng Y. and Cui L.,"Martensite fraction-temperature diagram of TiNi wires embedded in an aluminum matrix," *Intermetall.*, **12**, 1305–1309 (2004).

[5] Zheng Y., Cui L., Li Y. and Yand D., "Separation of the martensite in TiNi fiber reinforced aluminum matrix composite," *J. Mater. Sci. Technol.*, **20** (4), 390–394 (2004).

[6] Šittner P., Vokoun D., Dayananda G. N. and Stalmans R., "Recovery stress generation in shape memory Ti_{50} Ni_{45} Cu_5," *Mater. Sci. Eng. A*, **286**, 298–311 (2000).

[7] Vokoun D., Kafka V. and Hu C.T., "Recovery stresses generated by NiTi shape memory wires under different constraint conditions," *Smart Mater. Struct.*, **12**, 680–685 (2003).

[8] Rizzoni R. and Merlin M., "Deformation control of elastic thin layers by using shape memory wires," in preparation.

[9] Brinson L.C., "One Dimensional Constitutive Behavior of Shape Memory Alloys: thermomechanical derivation with non-constant material functions and redefined martensite internal variable," *J. Intell. Mat. Syst. Struct.*, **4** (2), 229–242 (1993).

[10] Kato H., Inagaki N. and Sasaki K., "A one-dimensional modelling of constrained shape memory effect," *Acta Mater.*, **52**, 3375–3382 (2004).

[11] Kosel F. and Videnic T., "Generalized plasticity and uniaxial constrained recovery in shape memory alloys," *Mech. Adv. Mater. Struct.*, **14**, 3–12 (2007).

[12] Briggs P. J. and Ponte Castañeda P., "Variational estimates for the effective response of shape memory alloy actuated fibre composites," *Journal of Applied Mechanics*, **69**, 470-480 (2002).

[13] Marfia S., "Micro-macro analysis of shape memory alloy composites," *International Journal of Solids and Structures*, **42**, 3677-3699 (2005).

[14] Marfia S. and Sacco E., "Micromechanics and homogenization of SMA-wire reinforced materials," *Journal of Applied Mechanics*, **72**, 259-268 (2005).

[15] De Simone A. and James R.D., "A constrained theory of magnetoelasticity," *J. Mech. Phys. Solids*, **50**, 283–320 (2002).

[16] James R.D. and Rizzoni R., "Pressurized shape memory thin films," *J. Elast.*, **59**, 399–436 (2000).

[17] Liu L.P., James R.D. and Leo P. H.,"Magnetostrictive composite in the dilute limit," *J. Mech. Phys. Solids*, **54**, 951–974 (2006).

[18] Zhou G. and Lloyd P., "Design, manufacture and evaluation of bending behaviour of composite beams embedded with SMA wires," *Comp. Sci. Technol.*, in press (2009).

[19] Le Dret H. and Meunier N., "Modeling heterogeneous martensitic wires," *Math. Models Methods Appl. Sci*, **15** (3), 375-406 (2005).

[20] Bhattacharya K., *Microstructure of martensite. Why it forms and how it gives rise to the shape-memory effect*, Oxford University Press (2003).